GLOBAL ACADEMIC RESEARCH INSTITUTE

COLOMBO, SRI LANKA

GARI International Journal of Multidisciplinary Research

ISSN 2659-2193

Volume: 08 | Issue: 04

On 31st December 2022

http://www.research.lk

Author: Nikita Rokan, Heshani Mudalige, Ominda Perera

School of Science, BMS, Sri Lanka

GARI Publisher | Pandemic | Volume: 08 | Issue: 04

Article ID: IN/ GARI/ICAS/2022/122 | Pages: 71-92 (22)

ISSN 2659-2193 | Edit: GARI Editorial Team

Received: 29.07.2022 | Publish: 31.12.2022

SITE SPECIFIC DOCKING FOR THE IDENTIFICATION OF EFFECTIVE PHYTOCHEMICALS AND THEIR BINDING SITES AGAINST SARS-COV-2

Nikita Rokan, Heshani Mudalige, Ominda Perera

School of Science, BMS, Sri Lanka

ABSTRACT

Coronavirus disease 2019 (COVID-19), induced SARS-CoV-2, has produced an unparalleled global health emergency, and continues to endanger society. Across the last two years, scientists from all over the world have worked tirelessly to improve our understanding of coronavirus biology. Alternative solutions are clearly needed since medication refinement and vaccination advancement necessitate significant time commitments. Based on the computer compatibility (Processor: 11th Gen Intel(R) Core (TM) i5-1135G7 @ 2.40GHz 2.42 GHz), Auto Dock suite 4.2.6 was utilized for site-specific docking. More importance has been made in recent years on discovering plant-derived chemicals that can be employed as effective therapeutics. Therefore, phytochemicals retrieved from NCBI PubChem were investigated and assessed their potential against the main protease of SARS-CoV-2 (PDB ID: 6LU7) which was downloaded from RCSB PDB. Clofazimine, an FDA authorized drug only for use in treatment of leprosy and a clinical trial drug for Covid-19 was provided as the standard. Best phytochemicals were retrieved centered on their binding energy (BE) and inhibition constant (Ki). BIOVIA Discovery Studio was employed to visualize best docking postures and interactions. Redocking (BE: -10.81 kcal/mol) was performed to validate docking methodology. Consequently, the most promising phytochemicals were identified as Ergosterol peroxide (BE: -10.00, Ki: 47.10), Robustaflavone (BE: -9.81, Ki: 64.21), Campesterol (BE: -9.18, Ki: 187.04), Rutin (BE: -8.84, Ki: 329.68) and Oleonolic acid (BE: -8.66, Ki: 451.45) kcal/mol and nM respectively. Absorption, distribution, metabolism, excretion, and toxicity (ADMET) properties were also investigated via ADMETlab 2.0. Ergosterol peroxide was picked as the best candidate since it did not violate the Lipinski rule and adhered to ADMET properties.

Key words: Covid-19, Site-specific, AutoDock suit 4.2.6, Phytochemicals, ADMETlab 2.0

INTRODUCTION

COVID-19 disease

Coronavirus disease-19 is a disease caused by a novel form of transmissible pathogenic human severe acute respiratory syndrome coronavirus-2 (SARS-CoV-2) which was first found in Wuhan, China (Al-Karmalawy et al., 2021). Later, COVID-19 has been classified as a pandemic by the WHO as of March 11, 2020 (Tallei et al., 2020). SARS-CoV-2 is a member of the subgenus Sarbecovirus, the genus Betacoronavirus, and the family Coronaviridae (Eweas, Alhossary and Abdel-Moneim, 2021).

As the virus has spread globally, with 565,207,160 confirmed cases and over 6,373,739 deaths as of 22 July 2022, and whereas in Sri Lanka, 664,704 individuals have died with 16,535 deaths (WHO, 2022).

Figure 1: Total number of cases in the world (WHO,2022)

Epidemiological studies have revealed that SARS-CoV-2 virus has a relatively low fatality rate (5%) but an elevated transmissibility rate (2–2.5%) than the previously learned coronaviruses MERS (34.4% fatality, 1% transmissibility) and SARS (9.5% fatality, 1.7–1.9% transmissibility). Serial viral load studies in COVID-19 patients using RT-qPCR revealed that the maximal viral load occurred during the first week of symptoms, with a median viral dropping time of 20 days. Antibody production begins around 10 days following the appearance of symptoms (Keretsu, Bhujbal and Cho, 2020).

A novel concept suggests that COVID-19 can be divided into three stages. Some medications are likely to be more effective in each phase independently. The viral early infection phase, the pulmonary phase, and the hyper-inflammation phase are the names given to these three stages. Antiviral medications are the best option in the early stages of illness. The lungs get implicated in the second phase because of the immune system's engagement. During this stage, several symptoms such as coughing, shortness of breath, and hypoxia are seen. Blood clots have also been seen, primarily in the second phase. The cytokine storm is generated by immune system activation during the hyper-inflammation phase. The cytokine storm impacts negatively on the lungs, kidneys, heart, and other organs (Zaim et al., 2020). During this stage, it is likely that the anti-inflammatory category of drug candidates should receive more attention (Molavi et al., 2021).

Protein-ligand docking

In this research protein-ligand docking studies can be utilized to simulate how potential drugs attach to a given 3D structure of a receptor, providing a score of binding energy (BE) value which characterizes the binding efficiency between ligand and target protein. There have already been successful applications that indicate how protein-ligand docking is becoming an effective instrument in pharmaceutical candidate development (Cava, Bertoli and Castiglioni, 2021).

Selection of protein receptor

The main protease of SARS-CoV-2 is 3-chymotrypsin-like protease (3CLpro). The 3CLpro aids in the viral replication, making it a good target for antiviral drugs. Protease inhibitors are effective at preventing coronavirus replication and proliferation by interfering with the post-translational processing of important viral polypeptides (Uzunova et al., 2020). Therefore, the analysis was based on an X-ray diffraction-based crystal structure of COVID-19 main protease in association with an inhibitor N3 with 2.16 Å resolution and no carbohydrate polymers

or chain splits (Peele et al., 2021). The SARS-CoV-2 crystal structure target protein (PDB ID: 6LU7) was acquired from Research Collaboratory for Structural Bioinformatics Protein Data Bank (RCSB PDB).

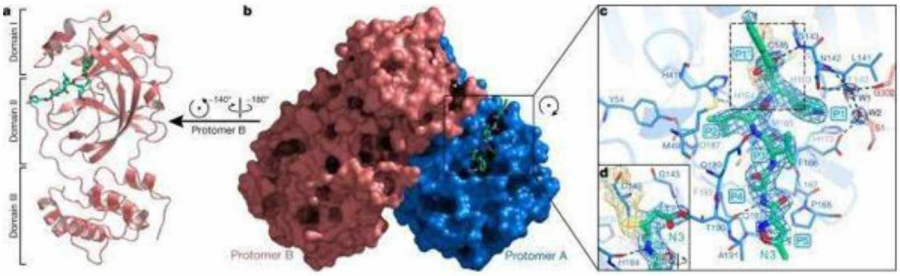

Figure 2: The crystal structure of SARS-CoV-2 $3CL^{pro}$ (PDB ID:6LU7) in complex with N3 (Jin *et al.*,2020)

Selection of ligands

Various literature reviews identified antiviral and antimalarial drugs as possible SARS-CoV-2 inhibitors. All the drugs utilized in this research have established pharmacokinetics and have been

U.S. Food and Drug Administration (FDA) approved for human use, therefore they do not have to go through long-term clinical studies, which can speed up the therapeutic development process (Mamidala et al., 2021) and can be used as positive controls to find out the best effective phytochemicals.

Table 1: *FDA approved drugs utilized in this study*

FDA Drug	PubChem ID	References
1. Amodiaquine	2165	Mamidala *et al.*, 2020.
2. Atovaquone	74989	
3. Halofantrine	37393	
4. Indinavir	5362440	
5. Maraviroc	3002977	Shamsi *et al.*, 2020.
6. Raltegravir	54671008	Molavi *et al.*, 2021.
7. Dexamethasone	5743	
8. Clofazimine	2794	Yuan *et al.*, 2020.
9. Nelfinavir	64143	Thangadurai *et al.*, 2020.

However, there are health consequences and hazardous effects associated with the use of these drugs. Safe and effective drugs with low adverse effects should be produced. Based on the facts presented above, the usage of herbal remedies and plant-based pharmacological compounds could be developed. They may be more useful and have less risks associated with drug applications. Therefore, phytochemicals with high bioactivity and low toxicity are perhaps the most effective alternative treatment (Sharanya, Sabu and Haridas, 2021).

Table 2: *Phytochemicals utilized in this study*

Phytochemical	PubChem ID	Sources	References
1. Kaempferol	5280863	Tea, Spinach, Beans	Sharanya, Sabu and Haridas, 2021.
2. Fisetin	5281614	Onions, Cucumbers, Strawberries	
3. Myricetin	5281672	Oranges, Tomatoes, Tea	Cherrak, Merzouk and Mokhtari-Soulimane, 2020.
4. Narirutin	442431		
5. Lonicerin	5282152	Fraser's sedge	
6. Hyperoside	5281643	Capillary wormwood	
7. Nicotiflorin	5318767	Hemp-agrimony	
8. Ergosterol peroxide	5351516	Wax gourd (Puhul), Linzhi mushroom	Thakur, Vadhera and Yadav, 2020.
9. Oleanolic acid	10494	Olives, Java-apple (Jambu)	
10. Campesterol	173183	Banana, Pomegranate	
11. Trifolin	5282149	Vigna mungo/ Black gram	Arora *et al*., 2020.
12. Quercitrin	5280459	White water lily	
13. Vitexin	5280441	Passion-flower,Bamboo leaves	
14. Baicalin	64982	Bark of Indian trumpet tree	
15. Syringetin	5281953	Red grapefruit	
16. Apigenin	5280443	Ginger	Thangadurai *et al*., 2020.
17. Luteolin	5280445		
18. Robustaflavone	5281694	Linn	Shivanika *et al*., 2022.
19. Rutin	5280805	Buckwheat, Asparagus	
20. Naringin	442428	Grapes, Citrus fruits	Imran *et al*., 2022.
21. Wogonin	5281703	Indian Trumpet Tree	
22. Rhein	10168	Aloe vera	Rameshkumar *et al*., 2020.
23. Astragalin	5282102	White fig	Hu *et al*., 2020.

The attraction of an exact ligand and asset whereby a ligand engages with and binds to the pocket of a target protein is referred to as BE. As a possible drug candidate, a medication with a lower BE is chosen (Mamidala et al., 2021). When a drug binds to a target protein, BE is defined as a decrease in the total energy of the complex.

Software's utilized

RCSB PDB and PubChem database were employed as online tools for data collection, evaluation, and analysis (Rahman et al.,2021). AutoDock 4.2.6 along with AutoDock Vina 1.1.2 is an open- source molecular docking software (Ravindranath et al., 2015). To visualize and analyse the 2D, 3D, and surface annotation of ligand interaction with the protein receptor BIOVIA Discovery

Studio 2021 (BIOVIA-DS), UCSF Chimera 1.16.1, and PyMOL 2.5 were used (Rahman et al., 2021).

Validation

The docking methods and parameters were confirmed by redocking experiments to verify that the ligand orientations and locations acquired from the experiments were relevant to understanding accurate and plausible candidate inhibitor binding modes (Al-Khodairy et al., 2013). This was tasked to guarantee that the inhibitor attaches to the active site gap precisely and with fewer deviation than co-crystallized complex (Shivanika et al., 2022).

The Ramachandran plot is an important aspect in evaluating the quality of protein 3D structures. It depicts the statistical distribution of possible backbone dihedral angle configurations between phi and psi (Wiltgen, 2018).

Significance of the study

From late 2019, the COVID-19 pandemic driven by SARS-CoV-2 has posed a serious worldwide health threat. To this day, there is no medicine that particularly targets and eradicates Covid-19. Several COVID-19 vaccines are currently being administered. Even though, it's still unclear whether they are effective against all COVID-19 strains and being vaccinated does not guarantee that COVID-19 will not reoccur. But it also claims reduction of the severe symptoms of COVID- 19 patients (Saha et al., 2021). A straightforward method in antiviral medication development is to use bioinformatics tools to screen already authorized chemical compounds. Medications are examined for their ability to suppress several crucial features of the new viruses using this approach (Molavi et al., 2021). Protein-ligand docking is utilized in this investigation to uncover appropriate ligands and their binding sites against SARS-CoV-2.

Materials

Table 3: *Utilized materials for the research*

Hardware	Software	Web sites
Device name: LAPTOP-CRI0HGRV Processor: 11th Gen Intel(R) Core (TM)i5-1135G7 @ 2.40GHz 2.42 GHz Installed RAM: 16.00 GB System type: 64-bit operating system,x64-based processor	Python 3.10.2 MGLtools 1.5.6 AutoDock suite 4.2.6 Open Babel GUI PyMOL 2.5 UCSF Chimera1.16 BIOVIA Discovery Studio2021	RCSB PDB NCBI Pubchem ZINC CASTp 3.0 PLIP ADMET lab 2.0 Ramachandran Analysis (https://saves.mbi.ucla.edu/)
Other		
Sri Lanka Telecom Wi-Fi Router-Fibre (100 mbps)		

Samples		
FDA approved drugs Phytochemicals		

METHODOLOGY

Receptor retrieval and preparation

The chosen receptor $3CL^{pro}$ (PDB ID: 6LU7) was retrieved from RCSB PDB in .pdb format. The 6LU7 receptor has two chains, A and C, that work together to create a homodimer. Chain A was employed, and Chain C was eliminated, which represented the complex-bound inhibitor to the protein receptor molecule. Water molecules were deleted. Then, polar hydrogens were added and Gasteiger charges were computed.

Ligand retrieval and preparation

The 3D Standard delay format (SDF) structure of all the ligands were acquired from NCBI Pubchem. SDF files were converted into .pdb format using the Open Babel GUI.

Site-specific docking (SSD) using AutoDock 4.2.6

The ligands were synthesized by determining missing atoms, rotatable bonds, and torsional degrees of freedom. The grid-box (Figure 4) was generated based on the receptor active sites predicted as in Hagar et al., 2020 literature review. GA was selected under search parameters option and Lamarckian genetic algorithm was selected under output option. Finally, autogrid.exe and autodock.exe were launched.

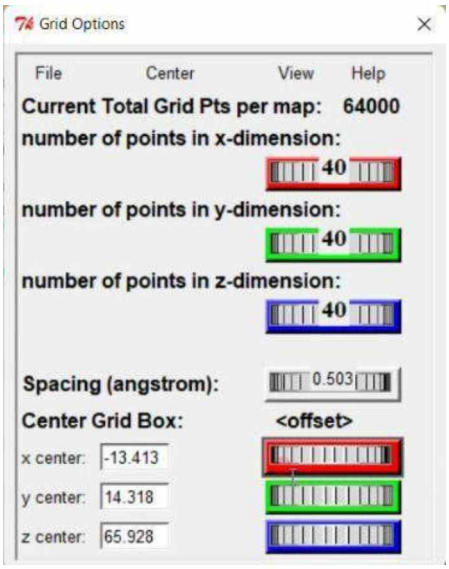

Figure 3: *SSD grid-box parameters*

Analysis of docking parameters

The docking simulation generated docking log files (.dlg) with Root mean square deviation (RMSD) table which contain docked protein-ligand complex conformations lowest BE and respective Ki values were analysed via AutoDock 4.2.6.

Visualization of docking poses

The finest docked poses were examined using the programs listed underneath.

Docked complex creation

For visualization of AutoDock SSD complexes had to be formed in Protein Data Bank, Partial Charge & Atom Type file (.pdbqt) format. This was created via AutoDock tools 4.2.6. Later,

.pdbqt format was converted into .pdb format by utilizing Open Babel GUI.

PyMOL

AutoDock 4.2.6 complex file was opened in .pdbqt format. To acquire the

highest image quality, necessary changes such as quality, colour space and background colour were applied.

Chimera

The ideal docked position in .pdbqt format was processed in Chimera, and a ribbon structure was shown as the complex. Furthermore, from preset menu 'Publication 3 mode' was selected and proceeded with needful colour amendments.

Analysis of Interactions

The hydrogen (HI) and hydrophobic (HPI) interactions for the respective poses docking were investigated using BIOVIA-DS. PDB files with the best docking pose was inspected. The 3D visualization, binding pockets, the forces, HIs and HPIs (Alkyl, Pi-Alkyl, Pi-Pi Stacked, Pi-Pi T-shaped, Amide-Pi Stacked, Pi-Sigma) were examined using docked 3D and 2D structures.

Analysis of ADMET properties

ADMET lab 2.0 was used to assess each phytochemical ligand's absorption, distribution,

metabolism, excretion, and toxicity (ADMET). Canonical SMILES were copied into ADMET lab

2.0 and ligand characteristics were investigated.

Validation

Redocking

PyMOL was used to isolate the co-crystallized natural ligand (N3 inhibitor) of the SARS-CoV-2 3CLpro complex 6LU7 structure, which was then used as the ligand. SSD as before in 2.2.6 was performed and results were analysed. RMSD value was computed after superimposing.

Ramachandran plot

By uploading respective PDB files, Ramachandran plots for 6LU7 and redocked complex were obtained through employing PROCHECK tool from the SAVES v6.0 server employing UCLA DOE lab website.

RESULTS

Docking Parameters

Based on the BE and Ki, possible SARS-CoV-2 3CLpro inhibitors were chosen When BE is lower, protein-ligand complex is steadier and lower the inhibition, suppression becomes better (Pantsar and Poso, 2018). Compounds with lowest BE and Ki values will be chosen as the most effective inhibitors

FDA Approved Drugs

Clofazimine, Maraviroc, and Indinavir exhibited a significantly negative BE values (-8.0 to -8.6 kcal/mol) and the lowest Ki values (22.55 to 240.97 nM).

Table 4: *SSD using AutoDock 4.2.6 results.*

Name	Binding Energy (kcal/mol)	Inhibition Constant (nM)
1. Clofazimine	-10.43	22.55
2. Maraviroc	-9.09	215.53
3. Indinavir	-9.03	240.97
4. Nelfinavir	-8.93	286.28
5. Atovaquone	-8.80	357.12
6. Raltegravir	-8.59	507.85
7. Halofantrine	-8.46	631.56
8. Amodiaquine	-7.94	1520
9. Dexamethasone	-7.68	2330

Phytochemicals

23 compounds for SSD were chosen regarding the exhibited best docking scores and were determined to be the optimal ligands at the protein's target site. Ergosterol peroxide,

Robustaflavone and Campesterol had the lowest BEs (-9.18 to -10.00 kcal/mol) and Ki values (0.04710 to 0.18704 µM).

Table 5: *SSD using AutoDock 4.2.6 results*

Name	Binding Energy (kcal/mol)	Inhibition Constant (µM)
1. Ergosterolperoxide	-10.00	0.04710
2. Robustaflavone	-9.81	0.06421
3. Campesterol	-9.18	0.18704
4. Rutin	-8.84	0.32968
5. Oleanolic acid	-8.66	0.45145
6. Quercitrin	-8.65	0.46031
7. Trifolin	-8.17	1.03
8. Baicalin	-8.05	1.25
9. Myricetin	-7.98	1.43
10. Naringin	-7.81	1.87
11. Fisetin	-7.70	2.26
12. Luteolin	-7.70	2.28
13. Kaempferol	-7.54	2.96
14. Narirutin	-7.52	3.06
15. Apigenin	-7.52	3.09
16. Astragalin	-7.46	3.41
17. Vitexin	-7.46	3.41
18. Syringetin	-7.23	5.05
19. Hyperoside	-7.23	5.06
20. Lonicerin	-7.18	5.44
21. Wogonin	-6.89	8.83
22. Nicotiflorin	-6.69	12.51
23. Rhein	-6.46	18.26

Best docked pose

Docking poses of FDA approved drugs by using Chimera

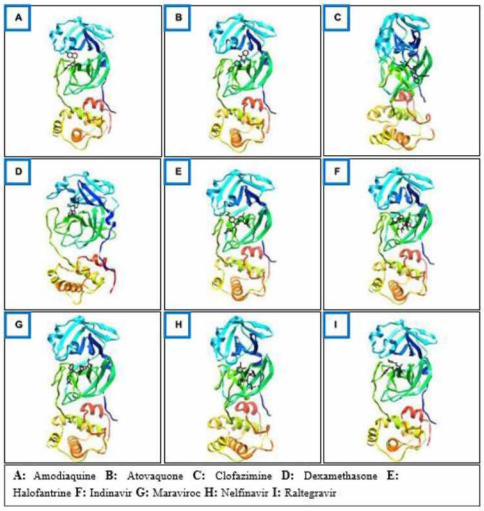

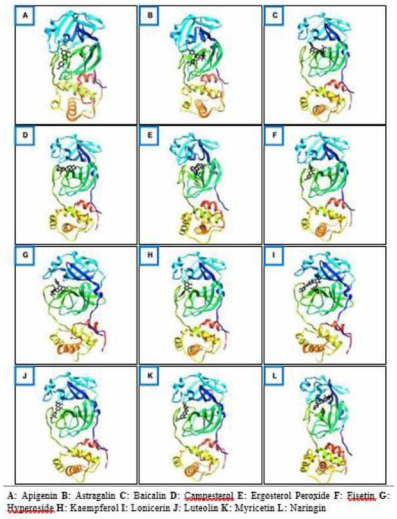

Figure 4: Ribbon diagrams (Ligand in black)

Docking poses of chosen phytochemicals by using Chimera

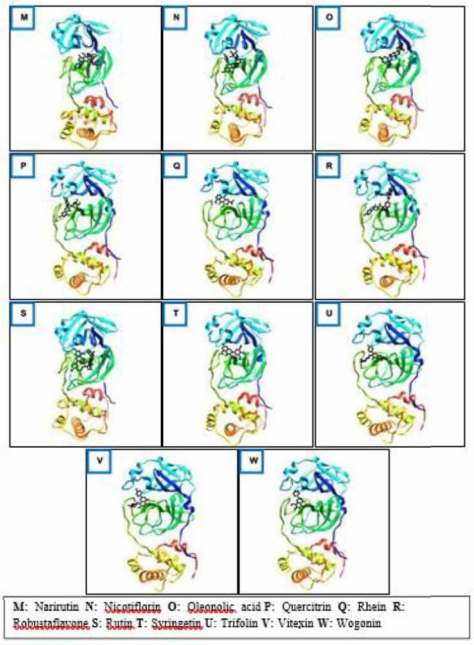

Figure 5: Ribbon Diagrams (Ligands in Black)

Protein-ligand interactions

Interactions plots and analysis using BIOVIA-DS of FDA approved drugs

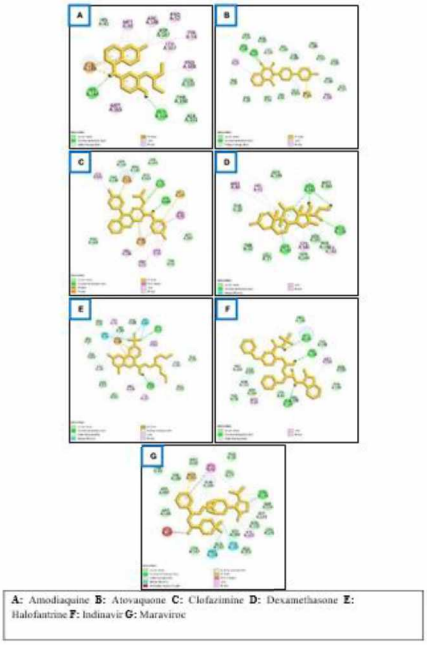

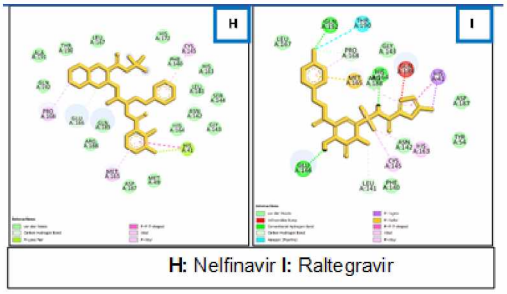

Figure 6: SSD interaction plots

Table 6: SSD amino acid (AA) residue interactions

Ligand	Interactions			
	HI		HPI	
	No.	Residue	No.	Residue
Amodiaquine	2	HIS164, GLU166	7	MET49, PRO52, TYR54, MET165, LEU167, PRO168, ARG188
Atovaquone	2	GLY143, SER144	2	LEU27, PRO168
Clofazimine	2	**CYS145,** HIS164	5	HIS41, MET49, PRO52, LEU141, ARG188,
Dexamethasone	3	ASN142, GLY143, GLU166	4	HIS41, MET49, **CYS145**, HIS163
Halofantrine	2	TYR54, GLU166	4	HIS41, MET165, LEU167, PRO168
Indinavir	3	HIS164, GLU166, GLN189	2	MET49, MET165
Maraviroc	1	CYS145	2	HIS41, HIS163
Molnupiravir	1	TYR54	2	MET49, PRO168
Nelfinavir	-	-	3	**CYS145**, MET165, PRO168
Oseltamivir	3	HIS164, THR190, GLN192	4	HIS41, MET49, MET165, PRO168
Raltegravir	3	HIS164, GLU166, GLN192	3	HIS41, **CYS145**, HIS163
Remdesivir	3	LEU141, ASN142, GLY143	4	HIS41, MET49, MET165, PRO168

HIS164 and GLU166 were the most common AA-residues involved in HIs which were on 5 compounds. Even though, Nelfinavir did not depict any number of HIs. HIS41, MET49 and PRO165 were the most common AA-residues involved in HPIs among 7 compounds. Also, MET165 was most common in between 6 compounds. CYS145 was present in both HIs and HPIs.

SSD interaction plots and analysis using BIOVIA-DS of phytochemicals

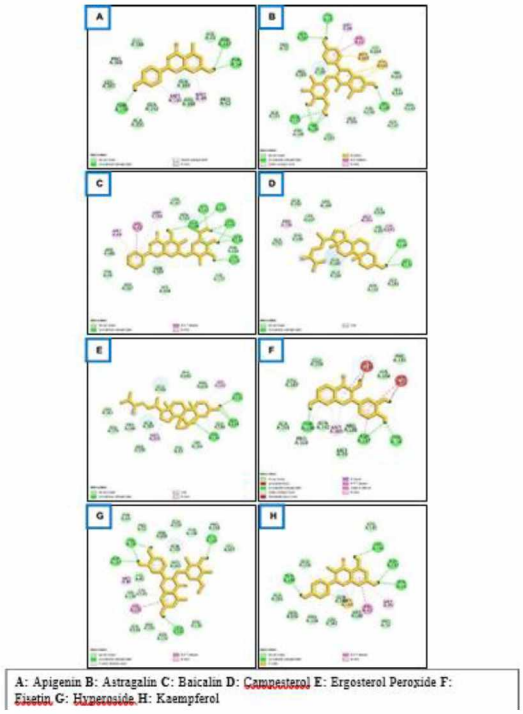

A: Apigenin B: Astragalin C: Baicalin D: Campesterol E: Ergosterol Peroxide F: Fisetin G: Hyperoside H: Kaempferol

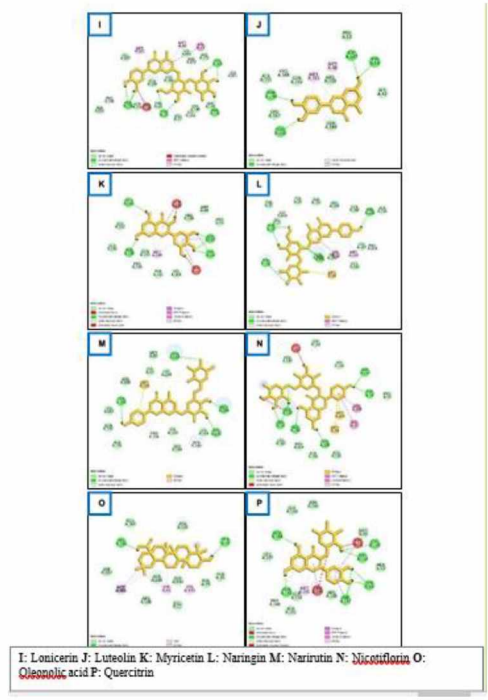

I: Lonicerin J: Luteolin K: Myricetin L: Naringin M: Narirutin N: Nicotiflorin O: Oleanolic acid P: Quercitrin

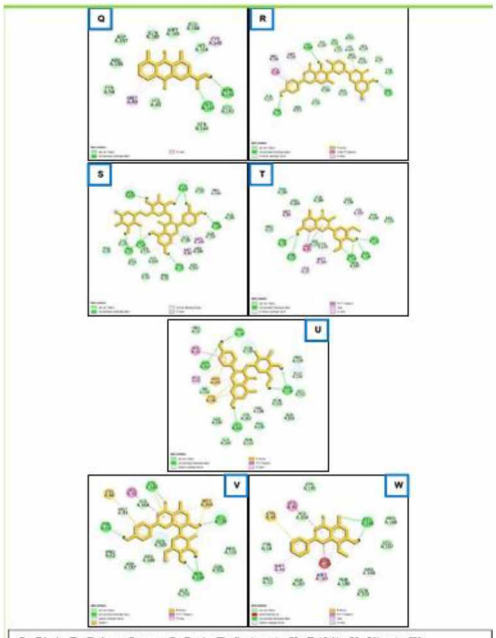

Q: Rhein R: Robustaflavone S: Rutin T: Syringetin U: Trifolin V: Vitexin W: Wogonin

Figure 7: SSD interaction plots

Table 7: SSD AA-residue

Ligand	Interactions			
	HI		HPI	
	No.	Residue	No.	Residue
Apigenin	3	TYR54, ASP187, THR190	2	MET49, MET165
Astragalin	5	TYR54, LEU141, ASP187, THR190, GLN192	2	HIS41, MET49
Baicalin	6	LEU141, GLY143, SER144, **CYS145**, **HIS163**, GLU166	3	HIS41, MET49, MET165
Campesterol	2	LEU141, SER144	3	**CYS145**, MET165, PRO168,
Ergosterol peroxide	3	LEU141, SER144, **CYS145**	2	**HIS163**, MET165
Fisetin	3	TYR54, ASP187, THR190	1	MET165
Hyperoside	4	TYR54, LEU141, GLU166, ASP187	2	MET49, **HIS163**
Kaempferol	4	TYR54, HIS164, ASP187, THR190	2	HIS41, MET49
Lonicerin	4	THR26, PHE140, **HIS163**, THR190	3	HIS41, MET49, MET165
Luteolin	4	TYR54, GLU166, ASP187, THR190	2	MET49, MET165
Myricetin	4	TYR54, GLU166, ASP187, THR190	1	MET165
Naringin	4	THR26, ASN142, **CYS145**, THR190	2	HIS41, MET165
Narirutin	4	PHE140, GLU166, **GLN189**, THR190	-	-
Nicotiflorin	6	SER46, TYR54, GLU166, ASP187, **GLN189**, THR190	2	HIS41, ARG188
Oleanolic acid	2	THR24, HIS164	4	HIS41, MET49, **CYS145**, MET165
Quercitrin	6	TYR54, **CYS145**, HIS164, GLU166, ASP187, THR190	1	MET165
Rhein	2	ASN142, GLY143	2	MET49, **CYS145**
Robustaflavone	3	THR26, HIS164, THR190	3	MET165, PRO168, **GLN189**
Rutin	6	**HIS41**, TYR54, ASN142, GLY143, GLU166, THR190	2	MET49, MET165
Syringetin	5	TYR54, LEU141, GLY143, SER144, ASP187	5	LEU27, HIS41, MET49, **HIS163**, MET165
Trifolin	4	TYR54, LEU141, ASP187, THR190	2	HIS41, MET49
Vitexin	4	TYR54, **CYS145**, GLU166, THR190	1	HIS41
Wogonin	1	GLU166	3	HIS41, MET49, MET165

THR190 was the most common AA-residue involved in HIs which were on 15 phytochemical compounds. Also, TYR54 and ASP187 AA-residues were involved in HIs 13 and 11 times respectively.

When analysing HPIs, MET 165 was found as the most common AA-residue which were on 15 compounds. HIS41 and MET49 were also notably in most of the compounds, 11 and 13 times accordingly. Additionally, Narirutin did not illustrate any HPI AA-residues. HIS41, CYS145, HIS163, GLN189 were common in both HIs and HPIs.

ADMET property analysis for phytochemicals

Since some of these substances are believed to be effective in inhibiting proteases, it is critical to understand the bioavailability and ADMET profiles of phytochemicals to utilize them safely and effectively. Lipinski's 'rule of five' is one method for weeding out chemicals with potential absorption issues (Ibrahim et al., 2020).

Table 8: Phytochemicals' ADMET properties determination

Name	Lipinski Rule	*Molecular Weight	nHA	logP	BBB Penetration	Caco-2 Permeability	HIA	AMES	H-HT
1. Apigenin	✓	270.05	5	3.307	x	-4.847	✓	(-)	x
2. Astragalin	X	448.1	11	-0.02	x	-6.105	(-)	✓	x
3. Baicalin	X	446.08	11	0.904	x	-6.34	x	x	x
4. Campesterol	✓	400.37	1	7.308	✓	-4.74	✓	x	x
5. Ergosterol peroxide	✓	428.33	3	6.012	**(-)	-4.756	✓	x	x
6. Fisetin	✓	286.05	6	2.428	x	-4.987	✓	✓	x
7. Hyperoside	X	464.1	12	-0.17	x	-6.206	x	✓	x
8. Kaempferol	✓	286.05	6	2.656	x	-4.974	✓	(-)	x
9. Lonicerin	X	594.16	15	-0.301	x	-6.304	x	✓	x
10. Luteolin	✓	286.05	6	2.902	x	-5.028	✓	(-)	x
11. Myricetin	✓	318.04	8	1.747	x	-5.653	✓	(-)	x
12. Narirutin	X	580.18	14	-0.591	x	-6.482	x	(-)	x
13. Naringin	X	580.18	14	-0.493	(-)	-6.501	x	(-)	x
14. Nicotiflorin	X	594.16	15	-0.553	x	-6.277	x	✓	x
15. Oleanolic acid	✓	456.36	3	6.486	(-)	-5.3	✓	x	x
16. Quercitrin	X	448.1	11	0.819	x	-6.142	(-)	✓	x
17. Rhein	✓	284.03	6	3.524	x	-5.232	✓	✓	x
18. Robustaflavone	X	538.09	10	6.077	x	-5.259	(-)	x	x
19. Rutin	X	610.15	16	-0.763	x	-6.336	x	✓	x
20. Syringetin	✓	346.07	8	2.463	x	-5.149	✓	(-)	x
21. Trifolin	X	448.1	11	-0.02	x	-6.105	(-)	✓	x
22. Vitexin	✓	432.11	10	0.33	x	-6.082	x	✓	x
23. Wogonin	✓	284.07	5	3.486	x	-4.884	(✓)	(-)	x

*Lipinski rule is acceptable (✓); Molecular Weight (Optimal Range-OR:100-600); nHA [number of hydrogen bond acceptors] (OR: 0 -12); logP [lipophilicity] (OR: ≤5.0); Caco-2 [Colon adenocarcinoma cell line] permeability (OR:>- 5.15log unit); HIA [Human Intestinal absorption] – Probability of absorption (✓); BBB [blood brain barrier] -

Probability of penetration (✓); AMES – Probability of being toxic (✓), H-HT [Human Hepatotoxicity] – probability of being toxic (✓) **(-) sign was added for moderate results in every characteristic

Remarkably, only 12 out of the 23 possible compounds examined above met Lipinski's rule. Also, Ergosterol peroxide which managed to get the lowest BE values in SSD adhered to Lipinski's rule. All the selected phytochemicals were negative for H-HT toxicity.

Validation

Redocking

SSD BE value = -7.76 kcal/mol (Ki value= 2.06 μM)

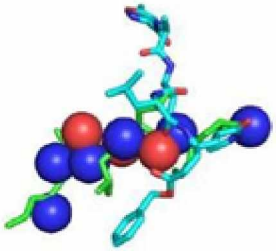

Figure 8: Superimposition of re-docked N3 and native co-crystallized N3 using PyMOL.

Following superimposition, RMSD value was 0.021 Å, which is lower than 2.0 Å (Majumdar and Mandal, 2020). This demonstrated the reliability of the docking technique.

Ramachandran plot

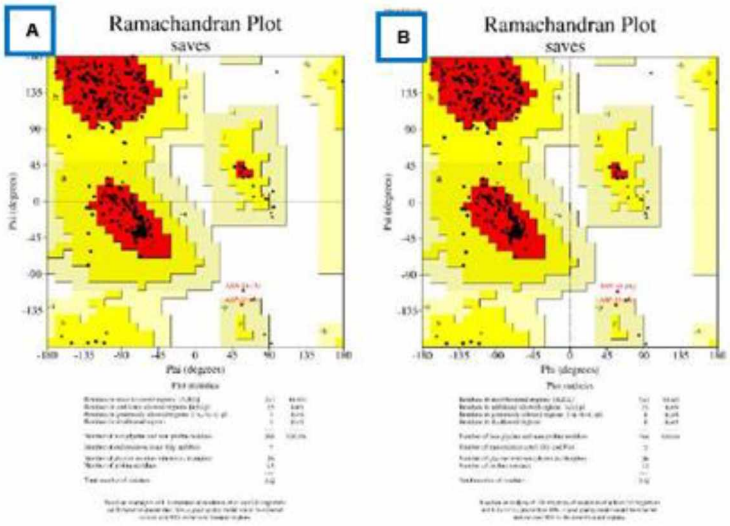

Figure 9: PDB ID: 6LU7-Ramachandran plots: A) Before docking B) After redocking

The number of residues in the most favourable areas (90.6%) remained the same before and after redocking, demonstrating that the docking process had no effect on the protein. As a result, the docking technique is legitimate (Wiltgen, 2018).

DISCUSSION

Molecular docking is among the most widely used approaches for identifying novel drug leads in the computer aided drug designing and now being used to swiftly annotate and evaluate large pharmacological libraries, saving enormous amounts of energy, time, and money (Rahman et al., 2021).

PDB ID: 6LU7, the 3CLpro in COVID-19, has been constructed and placed in PDB and has been publicly accessible from early February 2020. The 3CLpro of COVID-19 is 96% identical to the Mpro of SARS-CoV (Zhu et al., 2022). Prior to docking, the protein structure was arranged because on many occasions, the structure established by x-ray crystallographic research does not provide data on partial charges and hydrogen atoms, and certain residues could be lacking (Domagalski et al., 2014). In AutoDock 4.2.6, Gasteiger charges were utilized for each atom of the protein receptor instead of Kollman charges (Mamidala et al., 2021).

A GA is a type of search strategy based on Charles Darwin's theory of natural evolution. This algorithm is based on the natural selection process, in which the finest parties are preferred for reproduction to generate descendants of the following generation (Mallawaarachchi, 2017). GA settings were placed to 10 runs with 150 population size; 25,000,000 evaluations; 27,000 generation numbers with 0.02 default mutation rate and 0.8 crossover rate (Panikar et al., 2021).

Lamarckian genetic algorithm for ligand conformational incisive was employed which is a combination of GA and a native search algorithm. This technique first generates a population of entities, each of which is a different casual conformation of the docked enzyme. Local search method later accomplishes energy minimizations on a user-specified number of the population of individuals after each separate protein is changed to generate a varied translation and alternation. The entities with the lower subsequent energy are transmitted to the later generation, and the process is repeated. Also, each fresh collection of entities is permitted to get local search variants of their parents (Mamidala et al., 2021). H-bond formation among ligands and receptors is accountable for target-protein inhibition. It represents the strength of the protein-ligand connection (Hiremath et al.,2021). The stronger the bonds, the more hydrogen bonds produced with the AA-residue. This lowers the BE score and a low Ki which make the bonds extra stable (Tallei et al., 2021). Ki is a measurement of an inhibitor's efficacy and the compound concentration required to provide half-maximal inhibition of an enzyme (Georgakis et al., 2020).

Initially, the native co-crystal ligand: Inhibitor N3 of the 3CLpro complex was redocked to validate the accuracy of the virtual molecular docking methodology (Majumdar and Mandal, 2020). RMSD, which compares the structure of the docked receptor with a benchmark conformation, is used to determine the conformational changes that take place once the ligand connects with the receptor (Shukla and Singh, 2021).

Lipinski's rule does not consider the fact that most compounds serve as a substrate for at least one transporter, it cannot be utilized to assess a compound's drug-likeliness standalone (Bickerton et al., 2012). Therefore, BBB-penetration, Caco-2 permeability, HIA, AMES, H-HT

criteria were considered on ADMET analysis of phytochemicals as well.

BBB-penetration determines if substances can pass the blood-brain barrier. Since CNS-active drugs should avoid passing through it and inert CNS compounds must not cross it through to avoid CNS adverse effects (Panikar et al., 2021). Caco-2 cells are derived from human colon adenocarcinoma and include several drug transports routes, including the intestinal epithelium. The substances with modest intestinal epithelial absorption have anticipated Caco-2 values (Ahmed et al., 2020). The bioavailability expansion and amalgamation as determined by percentage of discharge/aggregate discharge in urine, bile, and faeces products is HIA information. HIA implies that the intestinal cell is capable of adequately absorbing the substances (Panikar et al., 2021). To assure the safety, toxicity evaluations must be validated. For that H-HT and AMES toxicity were evaluated to be non-carcinogenic (Mahmud et al., 2021).

Table 9: *Comparison of BEs from SSD of selected FDA-approved drugs*

Ligand	BE from this study (kcal/mol)	BE from Mamidala *et al.*, 2020 (kcal/mol)
Amodiaquine	-7.94	-8.65
Atovaquone	-8.80	-8.95
Halofantrine	-8.46	-8.68
Indinavir	-9.03	-10.00
Maraviroc	-9.09	-10.67
Raltegravir	-8.59	-7.81

Compared to previous study, the present study generated slightly higher BEs except for Raltegravir.

Table 4: AA residues comparison from SSD of selected FDA-approved drugs

Ligand	AA Residues from this study (kcal/mol)	AA residues from Mamidala et al., 2020 (kcal/mol)	Number of H-bonds interactions from this study	Number of H-bonds interactions from Mamidala et al., 2020
Amodiaquine	MET49, PRO52, TYR54, HIS164, MET165, GLU166, LEU167, PRO168, ARG188	HIS41, MET49, PHE140, LEU141, SER144, CYS145 HIS163, HIS164, MET165, GLU166, HIS172, ASP187, ARG188, GLN189, THR190, GLN192	2	2
Atovaquone	LEU27,	HIS41, CYS44,	2	1
	GLY143,	MET49, PRO52,		

	SER144,	TYR54, PHE140,		
	PRO168	LEU141, ASN142,		
		HIS163, HIS164,		
		MET165, GLU166,		
		HIS172, ASP187,		
		ARG188, GLN189		
Halofantrine	HIS41,	MET49, TYR54,	2	2
	TYR54,	LEU141, GLY143,		
	MET165,	SER144, CYS145,		
	GLU166,	HIS163, HIS164,		
	LEU167,	MET165 GLN189,		
	PRO168	THR190, ARG188,		
		GLU166, ASP187,		
		PRO168, LEU167,		
		GLN192		
Indinavir	MET49,	HIS41, MET49,	3	3
	HIS164,	PHE140, LEU141,		
	MET165,	ASN142, GLY143,		
	GLU166,	SER144, CYS145,		
	GLN189	HIS163, HIS164,		
		MET165, GLU166,		
		HIS172		
Maraviroc	HIS41,	HIS41, CYS44,	1	2
	CYS145,	MET49, TYR54,		
	HIS163	LEU141, ASN142,		
		GLY143, CYS145,		
		HIS164, MET165,		
		LEU167, PRO168,		
		ASP187,		
		ARG188, GLN189,		
		THR190, ALA191,		
		GLN192		
Raltegravir	HIS41,	HIS41, MET49,	3	3
	CYS145,	PHE140, LEU141,		
	HIS163,	ASN142, GLY143,		
	HIS164,	SER144, CYS145,		
	GLU166,	HIS163, HIS164,		
	GLN192	MET165, GLU166,		
		LEU167, PRO168,		
		HIS172, ARG188,		
		GLN189, THR190		

Except in Atovaquone all the mentioned FDA approved drugs had common AA residues. Atovaquone interacted with site residues that are not common with the referential study. Additionally, H-bonds were compared with the same study. Except in Maraviroc and Atovaquone, all the other compounds number of H-bonds were similar. Maraviroc had one H-bond less and Atovaquone had one H-bond more.

AutoDock suite has two major drawbacks. When utilizing large ligands, they have too many degrees of freedom and docking techniques cannot scan the available conformational space. Most of the time, breaking down the problem into smaller pieces is the best method to address it. Aside from selective side-chain mobility, the protein targets frequently exhibit substantial structural flexibility, which is not represented in the AutoDock suite (Forli et al., 2016).

CONCLUSION

From FDA approved drugs sample set, Clofazimine was chosen as the most potent candidate for positive control which is approved for use against mycobacterial infections and as an adjuvant therapy for multibacillary leprosy. It is already in use against COVID-19 patients and orally bioavailable, relatively inexpensive to manufacture making it an appealing clinical candidate for the treatment of COVID-19 outpatients and when merged with remdesivir in treatment for hospitalized patients (Yuan et al., 2020). In conclusion, Ergosterol peroxide out of the selected phytochemicals were chosen as the best choice since it showed the lowest BE and Ki values in SSD method. Also, it has adhered to Lipinski's rule and to the checked ADMET properties. Ergosterol peroxide is a naturally occurring steroid family compound that is present in many fungi and certain plants. It has anti-inflammatory, anticancer, antioxidant, and antiviral properties (Jeong and Park, 2020). To validate these results, more in-vitro and in-vivo clinical investigations are needed.

There are strategies that could be employed to maximize the study. AutoDock suite does not consider protein structural flexibility. As a result, for higher motions of loops/domains, the relaxed complex technique can be used with molecular dynamics and afterwards in docking simulations (Forli et al., 2016). Molecular docking and dynamic simulations will be used to investigate the inhibitor compounds' interactions with 3CLpro. Molecular dynamics simulations are well- established in-silico approaches for acquiring dynamic data at atomic spatial resolution (Cherrak, Merzouk and Mokhtar-Soulimane, 2020). In-silico studies are inadequate to prove the phytochemical efficacy. The primary steps in obtaining high-quality phytochemicals include selecting the suitable solvent, extraction, screening processes, fractionation, and identification. Polar and nonpolar solvents are extensively utilized in the plants' extraction. Maceration, digestion, decoction, Soxhlet extraction, superficial extraction, ultrasound-assisted and microwave-assisted extractions are all instances of extraction processes. The use of several chromatographic methods (Thin-layer, Gas, HPLC) allows for the fractionation and purification of phytochemical compounds. Finally, the identification techniques such as spectroscopy (mass, infrared, ultra- violet) are employed (Abubakar and Haque, 2020). Phytochemicals with possible inhibitors of pharmacological targets and could appear to be part of COVID-19 treatments following more cheminformatics and medical trials.

REFERENCES

Abubakar, A. R. and Haque, M. (2020) 'Preparation of Medicinal Plants: Basic Extraction and Fractionation Procedures for Experimental Purposes', Journal of pharmacy & bioallied sciences, 12(1), pp. 1–10. [Online] DOI: 10.4103/jpbs.JPBS_175_19 (Accessed: 28 July 2022).

Ahmed, I., Leach, D. N., Wohlmuth, H., De Voss, J. J. and Blanchfield, J. T. (2020) 'Caco-2 Cell Permeability of Flavonoids and Saponins from Gynostemma pentaphyllum: the Immortal Herb' ACS omega, 5(34), pp. 21561–21569. [Online] DOI: 10.1021/acsomega.0c02180 (Accessed: 23 July 2022).

Al-Karmalawy, A.A., Dahab, M.A., Metwaly, A.M., Elhady, S.S., Elkaeed, E.B., Eissa, I.H. and Darwish, K.M. (2021) 'Molecular Docking and Dynamics Simulation Revealed the Potential Inhibitory Activity of ACEIs Against SARS-CoV-2 Targeting the hACE2 Receptor', Frontiers in Chemistry, 9, pp. 1-21. [Online] DOI: 10.3389/fchem.2021.661230. (Accessed: 24 March 2022).

Al-Khodairy, F.M., Khan, M.K.A., Kunhi, M., Pulicat, M.S., Akhtar, S. and Arif, J.M. (2013) 'In Silico Prediction of Mechanism of Erysolin-induced Apoptosis in Human Breast Cancer Cell Lines' American Journal of Bioinformatics Research, 3(3), pp. 62-71. [Online] DOI: 10.5923/j.bioinformatics.20130303. 03 (Accessed: 24 March 2022).

Arora, S., Lohiya, G., Moharir, K., Shah, S. and Yende, S. (2020) 'Identification of Potential Flavonoid Inhibitors of the SARS-CoV-2 Main Protease 6YNQ: A Molecular Docking Study', Digital Chinese Medicine, 3(4), pp. 239–248. [Online] DOI: 10.1016/j.dcmed.2020.12.003 (Accessed: 12 June 2022).

Bickerton, G. R., Paolini, G. V., Besnard, J., Muresan, S. and Hopkins, A. L. (2012) 'Quantifying the chemical beauty of drugs', Nature chemistry, 4(2), pp. 90–98. [Online] DOI: 10.1038/nchem.1243 (Accessed: 07 June 2022).

Cava, C., Bertoli, G. and Castiglioni, I. (2021) 'Potential drugs against COVID-19 revealed by gene expression profile, molecular docking and molecular dynamic simulation', Future Virology, 16 (8), pp. 527–542. [Online] DOI: 10.2217/fvl-2020-0392 (Accessed: 14 March 2022).

Cherrak, S. A., Merzouk, H. and Mokhtari-Soulimane, N. (2020) 'Potential bioactive glycosylated flavonoids as SARS-CoV-2 main protease inhibitors: A molecular docking and simulation studies', PloS one, 15(10), pp. 1-14. [Online] DOI: 10.1371/journal.pone.0240653 (Accessed: 19 March 2022).

Domagalski, M. J., Zheng, H., Zimmerman, M. D., Dauter, Z., Wlodawer, A. and Minor, W. (2014) 'The quality and validation of structures from structural genomics', Methods in molecular biology, 1091, pp. 297–314. [Online] DOI: 10.1007/978-1-62703-691-7_21 (Accessed: 15 July 2022).

Eweas, A.F., Alhossary, A.A. and Abdel-Moneim, A.S. (2021) 'Molecular Docking Reveals Ivermectin and Remdesivir as Potential Repurposed Drugs Against SARS-CoV-2', Frontiers in Microbiology, 11, pp. 1-15. [Online] DOI: 10.3389/fmicb.2020.592908. (Accessed: 24 March 2022).

Forli, S., Huey, R., Pique, M. E., Sanner, M. F., Goodsell, D. S. and Olson, A. J. (2016) 'Computational protein-ligand docking and virtual drug screening with the AutoDock suite', Nature protocols, 11(5), pp. 905–919. [Online] DOI: 10.1038/nprot.2016.051 (Accessed: 14 July 2022).

Georgakis, N., Ioannou, E., Varotsou, C., Premetis, G., Chronopoulou, E. G. and Labrou, N. E. (2020) 'Determination of Half-Maximal Inhibitory Concentration of an

Enzyme Inhibitor', Methods in molecular biology, 2089, pp. 41–46. [Online] DOI: 10.1007/978-1-0716-0163-1_3 (Accessed: 26 July 2022).

Hagar, M., Ahmed, H. A., Aljohani, G. and Alhaddad, O. A. (2020) 'Investigation of Some Antiviral N-Heterocycles as COVID 19 Drug: Molecular Docking and DFT Calculations', International journal of molecular sciences, 21(11), pp. 1-3. [Online] DOI: 10.3390/ijms21113922 (Accessed: 26 June 2022).

Hiremath, S., Kumar, H., Nandan, M., Mantesh, M., Shankarappa, K. S., Venkataravanappa, V., Basha, C. and Reddy, C. (2021) 'In silico docking analysis revealed the potential of phytochemicals present in Phyllanthus amarus and Andrographis paniculata, used in Ayurveda medicine in inhibiting SARS-CoV-2', 3 Biotech, 11(2), pp. 1-18. [Online] DOI: 10.1007/s13205-020-02578-7 (Accessed: 17 June 2022).

Hu, X., Cai, X., Song, X., Li, C., Zhao, J., Luo, W., Zhang, Q., Ekumi, I. O. and He, Z. (2020) 'Possible SARS-coronavirus 2 inhibitor revealed by simulated molecular docking to viral main protease and host toll-like receptor', Future Virology, PubMed Central [Online]. Available at: https://www.ncbi.nlm.nih.gov/pmc/articles/PMC7295248/ (Accessed: 25 June 2022).

Ibrahim, Z. Y., Uzairu, A., Shallangwa, G. A. and Abechi, S. E. (2021) 'Application of QSAR Method in the Design of Enhanced Antimalarial Derivatives of Azetidine-2-carbonitriles, their Molecular Docking, Drug-likeness, and SwissADME Properties', Iranian journal of pharmaceutical research: IJPR, 20(3), pp. 254–270. [Online] DOI: 10.22037/ijpr.2021.114536.14901(Accessed: 07 June 2022).

Imran, M., Iqbal, S., Hussain, A., Uddin, J., Shahzad, M., Khaliq, T., Razzaq Ahmed, A., Mushtaq, L., Kashif, M. and Mahmood, K. (2022) 'In silico screening, SAR and kinetic studies of naturally occurring flavonoids against SARS CoV-2 main protease', Arabian journal of chemistry, 15(1), pp 1-16. [Online] DOI: doi.org/10.1016/j.arabjc.2021.103473 (Accessed: 19 May 2022).

Jeong, Y. U. and Park, Y. J. (2020) 'Ergosterol Peroxide from the Medicinal Mushroom Ganoderma lucidum Inhibits Differentiation and Lipid Accumulation of 3T3-L1 Adipocytes', International journal of molecular sciences, 21(2), pp. 1-13. [Online] DOI: 10.3390/ijms21020460 (Accessed: 06 May 2022).

Jin, Z., Du, X., Xu, Y., Deng, Y., Liu, M., Zhao, Y., Zhang, B., Li, X., Zhang, L., Peng, C., Duan,

Y., Yu, J., Wang, L., Yang, K., Liu, F., Jiang, R., Yang, X., You, T., Liu, X., Yang, X., Bai, F.,

Liu, H., Liu, X., Guddat, L.W., Xu, W., Xiao, G., Qin, C., Shi, Z., Jiang, H., Rao, Z. and Yang, H.

(2020) 'Structure of Mpro from SARS-CoV-2 and discovery of its inhibitors' Nature, 582, pp. 289– 293. [Online] DOI: 10.1038/s41586-020-2223-y (Accessed: 24 March 2022).

Keretsu, S., Bhujbal, S. and Cho, S. J (2020) 'Rational approach toward COVID-19 main protease inhibitors via molecular docking, molecular dynamics simulation and free energy calculation', Scientific Reports, 10(1), pp. 1-14. [Online] DOI: 10.1038/s41598-020-74468-0 (Accessed: 7 May 2022).

Mahmud, S., Paul, G. K., Afroze, M., Islam, S., Gupt, S., Razu, M. H., Biswas, S., Zaman, S., Uddin, M. S., Khan, M., Cacciola, N. A., Emran, T. B., Saleh, M. A., Capasso, R. and Simal-Gandara, J. (2021) 'Efficacy of Phytochemicals Derived from Avicennia officinalis for the Management of COVID-19: A Combined In Silico and Biochemical Study', Molecules (Basel, Switzerland), 26(8), pp. 1-18. [Online] DOI:

10.3390/molecules26082210 (Accessed: 21 May 2022).

Majumder, R. and Mandal, M. (2022) 'Screening of plant-based natural compounds as a potential COVID-19 main protease inhibitor: an in silico docking and molecular dynamics simulation approach', Journal of biomolecular structure & dynamics, 40(2), pp. 696–711. [Online] DOI: doi.org/10.1080/07391102.2020.1817787 (Accessed: 20 June 2022).

Mallawaarachchi, V. (2017) Introduction to Genetic Algorithms — Including Example Code. Available at: https://towardsdatascience.com/introduction-to-genetic-algorithms-including- example-code-e396e98d8bf3 (Accessed: 28 July 2022).

Mamidala, E., Davella, R., Gurrapu, S. and Shivakrishna, P. (2020) 'In Silico Identification of Clinically Approved Medicines Against the main Protease of Sars-Cov-2 – A Causative Agent of Covid-19', International Journal of Pharma and Bio Sciences, 11(1), pp. 107-122. [Online] DOI: 10.22376/ijpbs/lpr.2021.11.1.L107-122 (Accessed: 13 March 2022).

Molavi, Z., Razi, S., Mirmotalebisohi, S. A., Adibi, A., Sameni, M., Karami, F., Niazi, V., Niknam, Z., Aliashrafi, M., Taheri, M., Ghafouri-Fard, S., Jeibouei, S., Mahdian, S., Zali, H., Ranjbar, M.

M. and Yazdani, M. (2021) 'Identification of FDA approved drugs against SARS-CoV-2 RNA dependent RNA polymerase (RdRp) and 3-chymotrypsin-like protease (3CLpro), drug repurposing approach', Biomedicine & pharmacotherapy, 138, pp. 1-20. DOI: 10.1016/j.biopha.2021.111544 (Accessed: 19 June 2022).

Panikar, S., Shoba, G., Arun, M., Sahayarayan, J. J., Usha Raja Nanthini, A., Chinnathambi, A., Alharbi, S. A., Nasif, O. and Kim, H. J. (2021) 'Essential oils as an effective alternative for the treatment of COVID-19: Molecular interaction analysis of protease (Mpro) with pharmacokinetics and toxicological properties', Journal of infection and public health, 14(5), pp. 601–610. [Online] DOI: 10.1016/j.jiph.2020.12.037 (Accessed: 23 June 2022).

Pantsar, T. and Poso, A. (2018) 'Binding Affinity via Docking: Fact and Fiction', Molecules (Basel, Switzerland), 23(8), pp. 1-13. [Online] DOI: 10.3390/molecules23081899 (Accessed: 23 July 2022).

Peele, K. A., Chandrasai, P., Srihansa, T., Krupanidhi, S., Ayyagiri V.S., Babu, D. J., Indira, M., Reddy, A. R. and Venkateswarulu, T.C. (2020) 'Molecular docking and dynamic simulations for antiviral compounds against SARS-CoV-2: A computational study', Informatics in Medicine Unlocked, 19, pp. 1-6. [Online] DOI: 10.1016/j.imu.2020.100345 (Accessed: 25 March 2022).

Rahman, F., Tabrez, S., Ali, R., Alqahtani, A.S., Ahmed, M.Z. and Rub, A. (2021) 'Molecular docking analysis of rutin reveals possible inhibition of SARS-CoV-2 vital proteins', Journal of traditional and complementary medicine, 11(2), pp. 173-179. [Online] DOI: 10.1016/j.jtcme.2021.01.006. (Accessed: 28 July 2022).

Rameshkumar, M. R., Indu, P., Arunagirinathan, N., Venkatadri, B., El-Serehy, H. A. and Ahmad,

A. (2021) 'Computational selection of flavonoid compounds as inhibitors against SARS-CoV-2 main protease, RNA-dependent RNA polymerase and spike proteins: A molecular docking study', Saudi journal of biological sciences, 28(1), pp. 448–458. [Online] DOI: 10.1016/j.sjbs.2020.10.028 (Accessed: 25 June 2022).

Ravindranath, P.A., Forli, S., Goodsell, D.S., Olson, A.J. and Sanner, M.F. (2015) 'AutoDockFR: Advances in Protein-Ligand Docking with Explicitly Specified Binding Site Flexibility'

PLoS computational biology, 11(12), pp. 1-28. [Online] DOI: 10.1371/journal.pcbi.1004586. (Accessed: 18 May 2022).

Saha, S., Tanmoy, A, M., Tanni, A.A., Goswami, S., Sium, S.M.A., Saha, S., Islam, S., Hooda, Y.,

Malaker, A.R., Anik, A.M., Haq, M.S., Jabin, T,, Hossain, M.M., Tabassum, N., Rahman, H., Hossain, M.J., Islam, M.S. and Saha, S.K. (2021) 'New waves, new variants, old inequity: a continuing COVID-19 crisis', BMJ Global Health, 6(8), pp. 1-5. [Online] DOI: 10.1136/bmjgh-2021-007031. (Accessed: 26 March 2022).

Shamsi, A., Mohammad, T., Anwar, S., Al-Ajmi, M. F., Hussain, A., Rehman, M. T., Islam, A. and Hassan, M. I. (2020) 'Glecaprevir and Maraviroc are high-affinity inhibitors of SARS-CoV-2 main protease: possible implication in COVID-19 therapy', Bioscience reports, 40(6), pp. 1-8. [Online] DOI: 10.1042/BSR20201256 (Accessed: 19 March 2022).

Sharanya, C. S., Sabu, A. and Haridas, M. (2021) 'Potent phytochemicals against COVID-19 infection from phyto-materials used as antivirals in complementary medicines: a review', Future Journal of Pharmaceutical Sciences, 7(1) pp. [Online] DOI: 10.1186/s43094-021-00259-7 (Accessed: 19 March 2022).

Shivanika C, Deepak-Kumar S., Ragunathan, V., Tiwari, P., Sumitha, A. and Brindha-Devi,

P. (2022) 'Molecular docking, validation, dynamics simulations, and pharmacokinetic prediction of natural compounds against the SARS-CoV-2 main-protease', Journal of Biomolecular Structure and Dynamics, 40(2), pp. 585-611. [Online] DOI: 10.1080/07391102.2020.1815584 (Accessed: 18 March 2022).

Shukla, R. and Singh, T.R. (2021) 'High-throughput screening of natural compounds and inhibition of a major therapeutic target HsGSK-3 β for Alzheimer's disease using computational approaches',

Journal of Genetic Engineering and Biotechnology, 19(1), pp.1-17. [Online] DOI: 10.1186/s43141-021-00163-w (Accessed: 05 June 2022).

Tallei, T.A., Tumilaar, S.G., Niode, N.J., Fatimawali, F., Kepel, B.J., Idroes, R., Effendi, Y., Sakib,

S.A. and Emran,T.B. (2020) 'Potential of Plant Bioactive Compounds as SARS-CoV-2 Main Protease (Mpro) and Spike (S) Glycoprotein Inhibitors: A Molecular Docking Study', Scientifica, 2020, pp. 1-18. [Online] DOI: 10.1155/2020/6307457 (Accessed: 16 March 2022).

Thakur, L., Vadhera, P. and Yadav, N. (2020) 'COMBATING SARS-COV-19 BY PHYTOCHEMICALS: AN IN-SILICO STUDY, Innovare Journal of Life Sciences, 8(4), pp. 1-4. [Online]. Available at: https://innovareacademics.in/journals/index.php/ijls/article/view/38135 (Accessed: 12 June 2022).

Thangadurai, K., Rengasundari, G., Saravana P.S., Vithyavani, N., Sivasankari, K., Ramya, R., Jeeva R.G. and Kannan K.P. (2020) 'Molecular Docking Studies of Deva Chooranam against the Target Protein 6LU7 of Novel Corona Virus 2019', Indo Global Journal of Pharmaceutical Sciences, 10(2), pp. 19-25. [Online] DOI: 10.35652/IGJPS.2020.10204 (Accessed: 25 June 2022).

Uzunova, K., Filipova, E., Pavlova, V. and Vekov, T. (2020) 'Insights into antiviral mechanisms of remdesivir, lopinavir/ritonavir and chloroquine/hydroxychloroquine affecting the new SARS- CoV-2', Biomedicine & pharmacotherapy = Biomedecine & pharmacotherapie, 131, pp. 1-8. [Online] DOI: 10.1016/j.biopha.2020.110668 (Accessed: 25 March 2022).

Wiltgen, M (2018) 'Algorithms for Structure Comparison and Analysis: Homology Modelling of Proteins', Encyclopedia of Bioinformatics and Computational Biology, 1(2019), pp.

38-81. [Online] DOI: 10.1016/B978-0-12-809633-8.20484-6 (Accessed: 14 March 2022).

World Health Organization (2020) WHO Coronavorus (Covid-19) Dashboard. Available at: https://covid19.who.int/ (Accessed: 26 July 2022).

Yuan, S., Yin, X., Meng, X., Chan, J., Ye, Z., Riva, L., Pache, L., Chan, C., Lai, P., Chan, C., Poon,

V., Matsunaga, N., Pu, Y., Yuen, C., Cao, J., Liang, R., Tang, K., Sheng, L., Du, Y., Xu, W., Sze,

K., Zhang, J., Chu, H., Kok, K., To, K., Jin, D., Sun, R., Chanda, S. and Yuen, K. (2020) 'Clofazimine is a broad-spectrum coronavirus inhibitor that antagonizes SARS-CoV-2 replication in primary human cell culture and hamsters', Nature, 593(7859), pp.418–423. [Online] DOI: 10.1038/s41586-021-03431-4 (Accessed: 25 June 2022).

Zaim, S., Chong, J.H., Sankaranarayanan, V. and Harky, A. (2020) 'COVID-19 and Multi-Organ Response', Current Problems in Cardiology, 45(8), pp. 1-31 [Online] DOI: 10.1016/j.cpcardiol.2020.100618 (Accessed: 7 May 2022).

Zhu, J., Zhang, H., Lin, Q., Lyu, J., Lu, L., Chen, H., Zhang, X., Zhang, Y. and Chen, K. (2022) 'Progress on SARS-CoV-2 3CLpro Inhibitors: Inspiration from SARS-CoV 3CLpro Peptidomimetics and Small-Molecule Anti-Inflammatory Compounds', Drug design, development and therapy, 16, pp. 1067–1082. [Online] DOI: 10.2147/DDDT.S359009 (Accessed: 29 June 2022).